Remote Sensing Based Land Surface Temperature Analysis in Diverse Environment of Lalgudi Block

J. Ramachandran[1*], R. Lalitha[1] and K. Sivasubramanian[2]

[1]*Department of Soil and Water Conservation Engineering, Agricultural Engineering College and Research Institute, Tamil Nadu Agricultural University, Kumulur, Trichy, India.*
[2]*Office of Controller of Examination, Tamil Nadu Agricultural University, Coimbatore, India.*

Authors' contributions

This work was carried out in collaboration among all authors. All authors read and approved the final manuscript.

Original Research Article

ABSTRACT

Introduction: Land Surface Temperature (LST) is a significant climatic variable and defined as how hot the "surface" of the Earth would feel to the physical touch in a particular location. A spatial analysis of the land surface temperature with respect to different land use/cover changes is vital to evaluate the hydrological processes.
Methods: The objective of this paper is to assess the spatial variation of land surface temperature derived from thermal bands of the Landsat 8 Operational Land Imager (OLI) and the Thermal Infrared Sensor (TIRS) by using split window algorithm.
Place and Data: The study was conducted in Lalgudi block of Trichy District, Tamil Nadu, India. The block has diverse environment like forest area, barren land, river sand bed, water bodies, dry vegetation, cultivated areas (paddy, sugarcane, banana etc.) and settlements. Landsat 8 satellite images for four selected scenes (December 2014 & January 2015 and December 2017 & January 2018) were used to estimate the LST.
Results: The spatial and temporal variation of Normalized Difference Vegetation Index (NDVI) and LST were estimated. The average NDVI values of cropped fields varied from 0.3 to 0.5 in all the scenes. The maximum value of LST ranging from 35 to 40°C was recorded in river sand bed. Subsequently, semi-urban settlements in the central part of Lalgudi block exhibited higher

---

Corresponding author: E-mail: eeesurya.tnau@gmail.com;

temperature ranging from 28 – 30°C. The LST of paddy crop and sugarcane was in the range of 23 to 25°C. The water bodies exhibited LST around 20°C. The coconut plantations, forest area and *Prosopis juliflora* showed LST value ranging from 24 – 29°C. This kind of block level monitoring studies helps in adopting suitable policies to overcome or minimize the problems triggered by increase in land surface temperature.

ABBREVIATIONS

LST   : Land Surface Temperature
NDVI : Normalized Difference Vegetation Index
SW   : Split Window Algorithm
OLI   : Operation Land Imager
TIRS : Thermal Infrared sensor

1. INTRODUCTION

Land Surface Temperature (LST) is a significant climatic variable and defined as how hot the "surface" of the Earth would feel to the physical touch in a particular location [1]. It is the skin temperature of the earth surface that depends on the amount of sunlight received by any geographical area. Apart from sunlight, LST is also affected by the land cover, which leads to change in land surface temperature. The variations in land surface heat fluxes affect the ecological environment and hydrological processes [2]. It also has a direct impact on vegetation of that location.

LST plays a direct role in estimating long wave fluxes and an indirect role in estimating latent and sensible heat fluxes [3]. Soil moisture estimation [4] and evapotranspiration modeling [5] can be done based on LST for estimating the crop water requirement and planning efficient water management strategies in a regional scale. Hence knowledge on spatial and temporal variation of LST is essential.

With the advent of satellite images and digital image processing techniques, now it is possible to calculate spatial variation of LST. Landsat 8 satellite images comes with two different sets of images that are from the Operational Land Imager (OLI) sensor with nine bands (band 1 to 9) and Thermal Infrared sensor (TIRS) with two bands (band 10 and 11) [6]. These images help in mapping spatial extent, land surface temperature, vegetation cover and chemical composition of the surface.

Many researchers used different algorithms to estimate LST from remote sensing images [7] such as Split-Window algorithm (SW) [8,9], Dual Angle algorithm (DA) [10,11], Single-Channel algorithm (SC) [12,13]. An attempt was made to detect the change of land surface temperature in relation to land use land cover change and fractal vegetation cover in some selected phases at English Bazar Municipality of Malda, West Bengal, India [14]. The study also investigated the temperature characters in different vegetation density zones, water depths, built up zones over selected time periods. A study was conducted to assess the impact of land cover change (LCC) on LST, using Landsat TM 5, Landsat 8 TIRS/OLI and Digital Elevation Model (ASTER) for Spiti Valley, Himachal Pradesh, India [15]. Land surface temperature in relation to Land use types and geological formation in northeast Jordan using split-window algorithm was estimated [16]. A review about the progress in estimation of LST from TIR and suggested directions for future research on the subject was presented [17].

This study attempts to analyze the spatial variation of land surface temperature by using split-window algorithm from Landsat 8 satellite images for various land use/cover in Lalgudi block.

2. MATERIALS AND METHODS

2.1 Study Area

Lalgudi block, located at Tiruchirapalli District, Tamil Nadu, India was selected for this study. The latitude 10.87 and longitude 78.83 are the geo-coordinate of the Lalgudi block (Fig. 1). The northern part of Lalgudi block has dense dry vegetation and barren lands. The southern part is bounded by River Coleroon. The Lalgudi Town is located at the central part of the block. Most of the inner part of the Lalgudi has cultivated areas where paddy, sugarcane, banana and other vegetables are grown.

2.2 Image Selection

Landsat 8 is the most recently launched satellite of the Landsat series. The Landsat 8 satellite images were downloaded from the USGS Earth Explorer website. To maintain homogeneity in dataset, two pairs of images of December 05,

2014 & January 22, 2015 and December 29, 2017 & January 30, 2018 were acquired. The period of images taken was based on paddy cultivation season. Table 1 presents image acquisition date, solar elevation angle and zenith angle for the Landsat 8 data products used. The projection of satellite images is Universal Traverse Mercator (UTM) and the UTM zone of satellite images used is as follow as: UTM_ZONE = 44. The path and row of satellite pass is 143 and 52 respectively. The images were selected such that there is no or minimum cloud cover (Table 1) in order to avoid error.

2.3 Computation of Land Surface Temperature (T_s)

Land Surface temperature (T_s) is an important parameter in understanding the exchange of energy between the earth surface and the environment. LST was calculated from the thermal band (band 10 and 11) radiance values of the Landsat 8 image. The equation for estimation of surface temperature is as follow:

$$T_s = \frac{K_2}{\ln\left(\dfrac{\varepsilon_s * K_1}{\rho_b}\right)} \qquad (1)$$

The radiance ρ_b of the thermal band (band 10) was calculated from Equation 2. The constants K_1 and K_2 for band 10 are 774.8853 and 1321.0789 which was taken from the metadata file. The surface emissivity (ε_s) was calculated

from equation 3. The radiance (ρ_b) was calculated from the pixel values of different bands (DN_b) using the following equation:

$$\rho_b = Add_{rad,b} + \left(Mult_{rad,b} * DN_b\right) \qquad (2)$$

where $Add_{rad,b}$ is additive and $Mult_{rad,b}$ is multiplicative terms related to different band radiance. The values of Add_{rad} and $Mult_{rad}$ terms of band 10 are 0.10000 and 3.3420E-04.

Surface emissivity (ε_s) is the ratio of the thermal energy radiated by the surface to the thermal energy radiated by a blackbody at the same temperature. It is given by:

$$\varepsilon_s = \begin{cases} 1.009 + 0.047\left(\ln\left(NDVI\right)\right) \rightarrow \left(NDVI > 0\right) \\ 1 \rightarrow \left(NDVI < 0\right) \end{cases} \qquad (3)$$

Thus, the surface emissivity was empirically derived from NDVI. NDVI is the ratio of difference in reflectivity of near-infrared (NIR) band and red band to their sum. The expression for estimation of NDVI is given by

$$NDVI = \frac{NIR - RED}{NIR + RED} \qquad (4)$$

In Landsat 8 image, the near infrared is band 5 and the red is band 4. Using Raster Calculator tool in ArcGIS, NDVI raster was obtained.
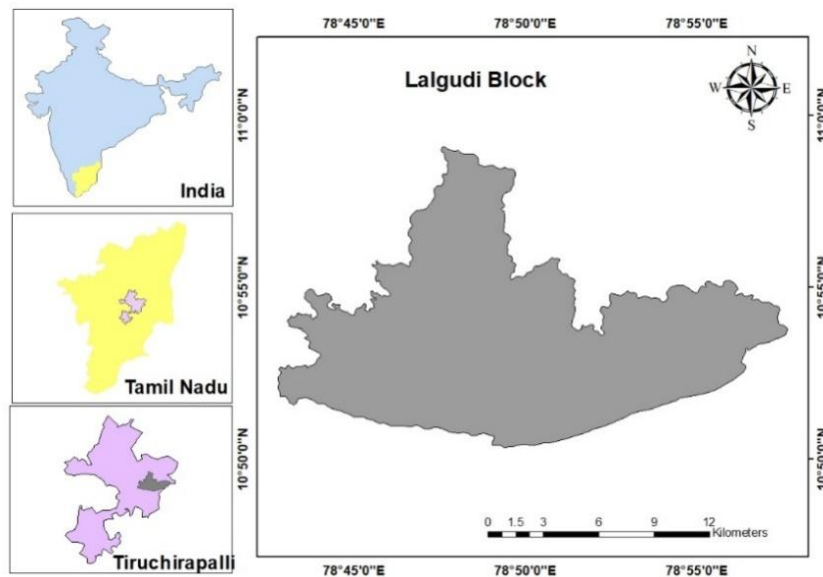
Fig. 1. The location of study area – Lalgudi Block

Table 1. Meta data of Landsat 8 image used

S. No.	Acquisition date (yyyy/mm/dd)	Solar elevation angle (degrees)	Solar azimuth angle (degrees)	Cloud cover in image (%)	Cloud cover in study area (%)
1	2014-12-05	49.38	146.60	2.46	0.77
2	2015-01-22	48.22	138.31	0.01	0.00
3	2017-12-29	47.08	144.18	23.15	0.40
4	2018-01-30	49.39	135.62	0.17	0.00

Source: Metadata file downloaded along with the Landsat 8 Image

A ground truth survey was conducted to identify the present land use/cover in Lalgudi block during the month of September, October and November, 2018. The previous year land use/cover details was collected through interview with the farmers during the time of survey. The latitude and longitude of the places visited, was also noted using a Global Positioning System (GPS). A point shapefile was prepared in ArcGIS using the latitude, longitude and land use/cover collected at the survey. The LST values for the known land use/cover points were extracted to those points, from the spatial map of LST, estimated from the above stated algorithm. Using that point LST values, the variation of LST for each land use/cover were compared graphically.

3. RESULTS AND DISCUSSION

The spatial and temporal variation of NDVI and LST are presented in Fig. 2 and 3 respectively for the four selected scenes. The southern part of the study area is bounded by the River Coleroon and hence negative values of NDVI was observed in the southern part of all the scenes (Fig. 2). The NDVI values for water bodies ranges from -0.07 to -0.09 [18]. The river sand bed and standing water in the pits resulted in negative values of NDVI in the southern part. Subsequently, the LST was higher in the river sand bed and comparatively lesser in the pits with standing water. This is clearly indicated in the images by pale yellow color patches in the southern part of LST maps (Fig. 3). Similarly, the LST was higher in the northern part (Fig. 3) where barren land and dry vegetation exists. The dry vegetation includes cactus, prosopis etc. Likewise, fallow land exhibited a maximum LST (29.2°C) in the study conducted at Malda [14]. The LST value of a lake located in the eastern part of Lalgudi was around 20°C when water is available (Fig. 3a and 3b). The LST increased in December 2017 (Fig. 3c) and January 2018 (Fig. 3d) images because of the presence of water weeds on the surface of water. The value of NDVI also simultaneously increased for the lake in those respective scenes (Fig. 2c and 2d). It was reported that the LST of water bodies was higher compared to LST of water hyacinth [14].

The scenes used in this study falls in the active tillering (December 2017), panicle initiation (December 2014 and January 2018) and dough stage (January 2015) of samba season paddy crop respectively. In all stages of paddy, the LST was in the range of 23 to 25°C. Similarly LST of sugarcane was also in the range of 23 – 25°C. The average NDVI values of sugarcane and banana fields varied from 0.3 to 0.5 in all the scenes.

In December 2017 and January 2018 scenes, the LST of Banana was comparatively higher than LST in December 2014 and January 2015 scenes (Fig. 4) because, in December 2017 and January 2018, there existed newly planted banana plants. The combined effect of soil and young banana plants was the reason behind the increase in LST. The coconut plantations, forest area and *Prosopis juliflora* exhibited similar trend (Fig. 4) of LST value ranging from 24 – 29°C. This was greater when compared to LST of the paddy crop.

The semi-urban settlements in the central part of Lalgudi block exhibited higher temperature (28 – 30°C) compared to the cropped surface. It was also reported that a dominant built up land experienced LST greater than 31.5°C [14]. The maximum value of LST ranging from 35 to 40°C was recorded in the river sand bed. Similarly it was noticed that asphalt and concrete gave the highest surface temperatures, while vegetated surfaces gave the lowest [19]. Bare soil gave surface temperatures that lie between those for pavements and plant-covered surfaces [19].
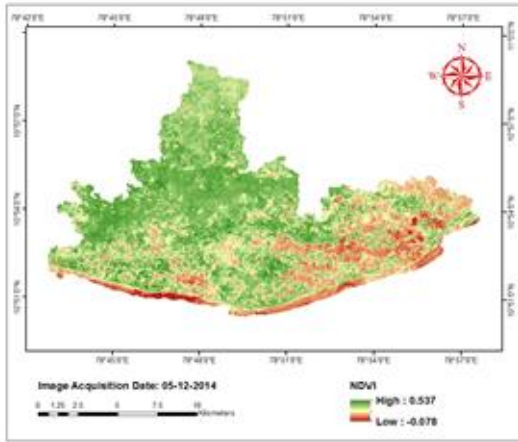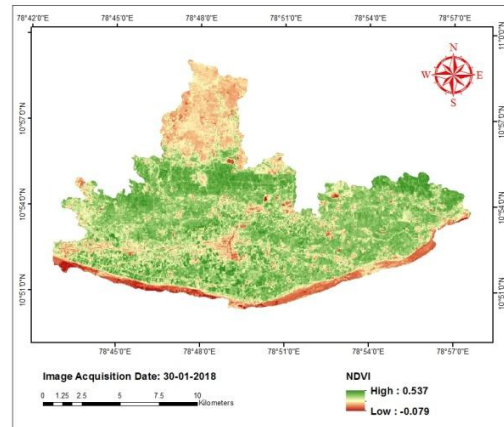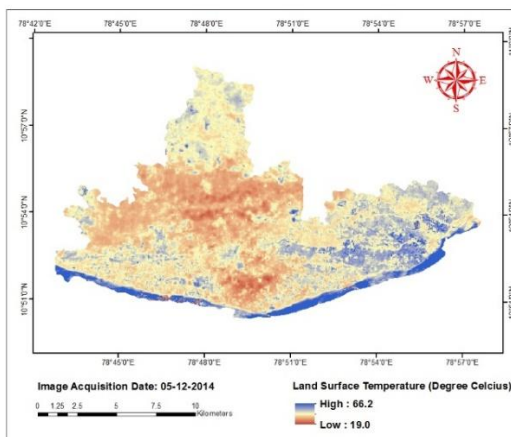
a) December 2014
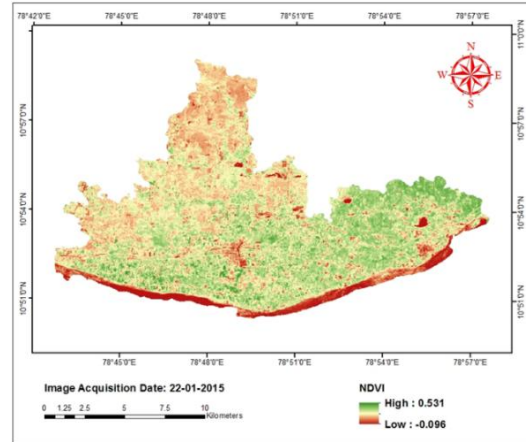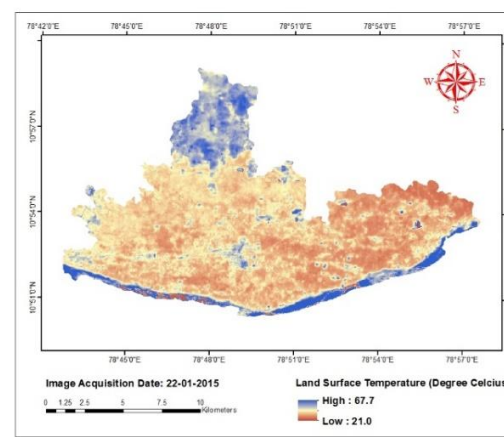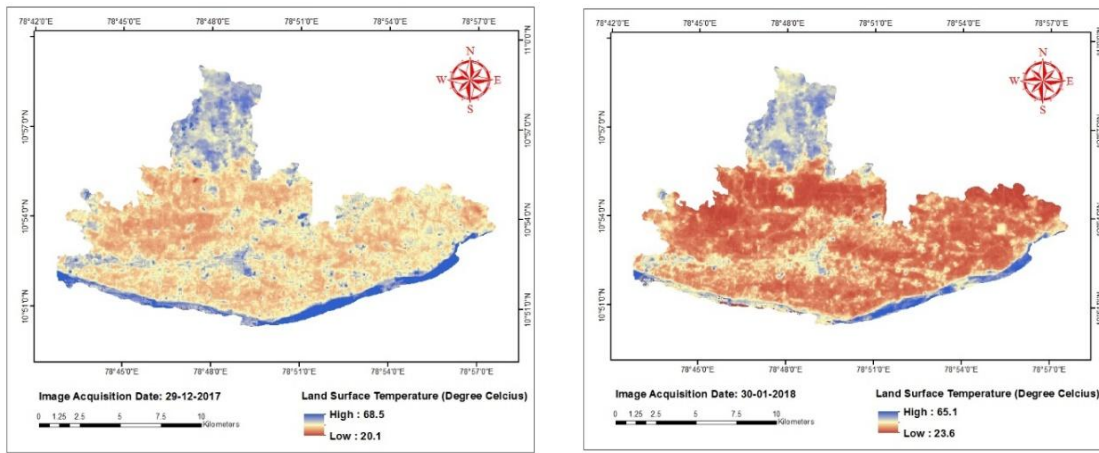
b) January 2015
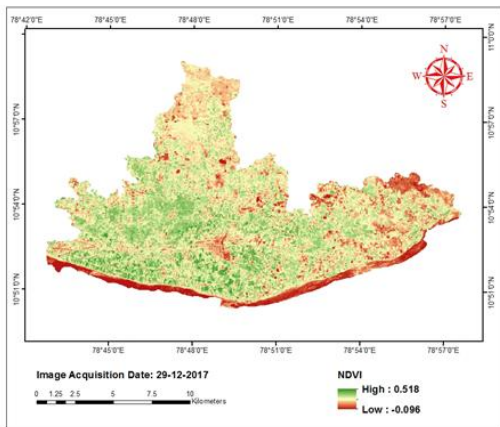
c) December 2017

d) January 2018

Fig. 2. Spatio-temporal variation of NDVI in Lalgudi block

a) December 2014

b) January 2015

c) December 2017   **d) January 2018**

Fig. 3. Spatio-temporal variation of LST in Lalgudi block
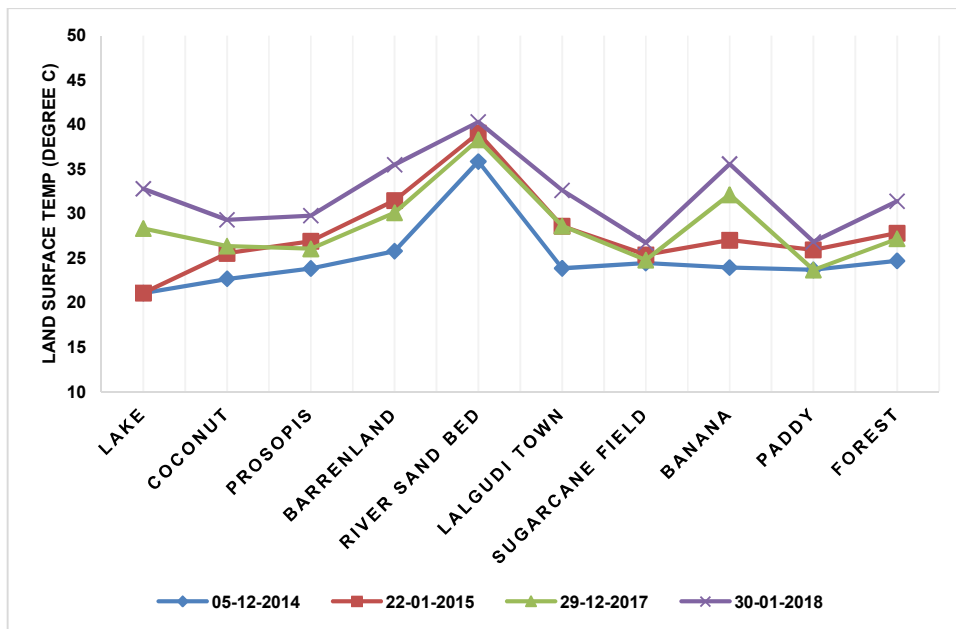

Fig. 4. LST variation of different surfaces in lalgudi block

4. CONCLUSION

A mathematical approach was used to estimate the LST from brightness temperature calculated from thermal bands of TIRS sensor and land surface emissivity and NDVI derived from optical bands of OLI sensor. LST was diversified due to positional influence of the existing land use/cover of Lalgudi block. A discrete difference in LST was identified in different land use/cover. The transformation of wetland into urban land, exchange of land between orchard and agricultural land etc. are some vital causes behind land surface temperature change which may be avoided. Green belt can be implemented in the areas having higher land surface temperature. This kind of block level monitoring studies helps in adopting suitable policies to overcome or minimize the problems triggered by increase in land surface temperature.

ACKNOWLEDGEMENT

COMPETING INTERESTS

Authors have declared that no competing interests exist.

REFERENCES

1. European Space Agency. User Guide for Sentinel 3; 2019.
   Available:https://sentinel.esa.int/web/sentinel/user-guides/sentinel-3-slstr/overview/geophysical-measurements/land-surface-temperature

2. Hu G, Zhao L, Wu RLX, Wu T, Zhu X, Pang Q, Liu GY, Du E. Simulation of land surface heat fluxes in permafrost regions on the Qinghai-Tibetan Plateau using CMIP5 models. Atmospheric Research; 2019.

3. Bastiaanssen WGM, Menenti M, Feddes RA, Holslag AAMA. Remote sensing surface energy balance algorithm for land (SEBAL) – formulation. Journal of Hydrology. 1998;198-212.

4. Price JC. The potential of remotely sensed thermal infrared data to infer surface soil moisture and evaporation. Water Resources. 1990;16:787-795.

5. Silva BB, Mercante E, Boas MAV, Wrublack SC, Oldoni LV. Satellite-based ET estimation using Landsat 8 images and SEBAL model. Revista Ciência Agronômica. 2018;49(2):221-227.

6. Roy DP, Wulder MA, Loveland TR, Woodcock CE, Allen RG, Anderson MC, Helder D, Irons JR, Johnson DM, Kennedy R, Scambos TA, Schaaf CB, Schott JR, Sheng Y, Vermote EF, Belward AS, Bindschadler R, Cohen WB, Gao F, et al. Landsat-8: Science and product vision for terrestrial global change research. Remote Sensing of Environment. 2014;145:154–172.

7. Latif MS. Land surface temperature retrieval of landsat-8 data using split window algorithm-A case study of Ranchi district. International Journal of Engineering Development and Research. 2014;2:3840-3849.

8. Atitar M, Sobrino JA. A split-window algorithm for estimating LST from Meteosat 9 data: Test and comparison with in situ data and MODIS LSTs. IEEE Geoscience and Remote Sensing Letters. 2009;6:122–126.

9. Jiménez-Muñoz JC, JA, Sobrino D, Skoković C. Mattar, Cristóbal J. Land surface temperature retrieval methods from landsat-8 thermal infrared sensor data. IEEE Geoscience and Remote Sensing Letter. 2014;11(10):1840–1843.

10. Prata AJ. Surface temperatures derived from the advanced very high resolution radiometer and the along track scanning radiometer. 1. Theory. Journal of Geophysical Research. 1993;98:16689–16702.

11. Sobrino JA, Li ZL, Stoll MP, Becker F. Multi-channel and multi-angle algorithms for estimating sea and land surfaces temperature with ATSR data. International Journal of Remote Sensing. 1996;17:2089–2114.

12. Cristóbal J, Jiménez-Muñoz JC, Prakash A, Mattar C, Skoković D, Sobrino JA. An improved single-channel method to retrieve land surface temperature from the landsat-8 thermal band. Remote Sensing. 2018;10(3):431.

13. Duan SB, Li ZL, Wang C, Zhang S, Tang BH, Leng P, Gao MF. Land-surface temperature retrieval from landsat 8 single-channel thermal infrared data in combination with NCEP reanalysis data and ASTER GED product. International Journal of Remote Sensing. 2018;1–16.

14. Pal S, Ziaul S. Detection of land use and land cover change and land surface temperature in English Bazar urban centre. The Egyptian Journal of Remote Sensing and Space Science. 2017;20(1):125–145.

15. Kumar P, Husain A, Singh RB, Kumar M. Impact of land cover change on land surface temperature: A case study of Spiti Valley. Journal of Mountain Science. 2018;15(8):1658-1670.

16. Ibrahim M, Abu-Mallouh H. Estimate land surface temperature in relation to land use types and geological formations using spectral remote sensing data in northeast Jordan. Open Journal of Geology. 2018;8:174-185

17. Li ZL, Tang BH, Wu H, Ren H, Yan G, Wan Z, Trigo IF, Sobrino JA. Satellite-derived land surface temperature: Current

status and perspectives. Remote Sensing of Environment. 2013;131:14–37.

18. Lillesand TM, Kiefer RW, Chipman JW. Remote sensing and image interpretation. Hoboken, NJ: John Wiley & Sons; 2008.

19. Herb WR, Janke B, Mohseni O, Stefan HG. Ground surface temperature simulation for different land covers. Journal of Hydrology. 2008;356(3-4):327–343.

Peer-review history:
The peer review history for this paper can be accessed here:
http://www.sdiarticle3.com/review-history/48767